unpaired electron are twice removed from the aromatic rings and this is in agreement with the small isotropic hyperfine splitting, 1.3 MHz, for these closest protons. Ring protons in polynuclear hydrocarbons such as anthracene and tetracene have a minimum splitting of 3 MHz. Such large splittings have not been observed in the ENDOR spectra of SRC and raw coal.

This study has also helped to evaluate the range of applicability of the new improved model for the matrix ENDOR response in disordered systems.[9] The experimental variation of line shape, line width, and intensity of the matrix ENDOR line is reproduced very well as a function of both the microwave and radio-frequency field intensities for microwave powers up to that which gives the maximum ENDOR response. The deviation of the experimental spectra from the simulated ones at high microwave power may be related to the approximation that the relaxation parameters are independent of the microwave field. The satisfactory agreement of the theory with the experimental spectra at low and medium microwave powers lends confidence in its ability to give new and useful structural information about paramagnetic species in disordered solids.

Acknowledgment. This work was supported by the U.S. Army Research Office and the Wayne State University Computing Center. We thank Dr. L. T. Taylor for drawing our attention to this coal sample and Drs. D. Becker and J. Michalik for the measurement of T_{1e}.

References and Notes

(1) R. S. Alger, "Electron Paramagnetic Resonance: Techniques and Applications", Wiley-Interscience, New York, N.Y., 1968, p 416, and references cited therein.
(2) J. Uebersfeld, A. Etienne, and J. Combrisson, *Nature (London)*, **174**, 614 (1954).
(3) H. L. Retcofsky, G. P. Thompson, R. Raymond, and R. A. Friedel, *Fuel*, **54**, 126 (1975).
(4) H. L. Retcofsky, J. M. Stark, and R. A. Friedel, *Anal. Chem.*, **40**, 1699 (1968).
(5) D. L. Wooton, H. C. Dorn, L. T. Taylor, and W. M. Coleman, *Fuel*, **55**, 224 (1976).
(6) L. T. Taylor, private communication.
(7) See, for instance, L. Kevan and L. D. Kispert, "Electron Spin Double Resonance Spectroscopy, Wiley-Interscience, New York, N.Y., 1976.
(8) (a) J. Helbert, L. Kevan, and B. L. Bales, *J. Chem. Phys.*, **57**, 723 (1972); (b) J. Helbert and L. Kevan, *ibid.*, **58**, 1205 (1973); (c) B. L. Bales, R. N. Schwartz, and L. Kevan, *Chem. Phys. Lett.*, **22**, 13 (1973); (d) R. N. Schwartz, M. K. Bowman, and L. Kevan, *J. Chem. Phys.*, **60**, 1690 (1974); (e) H. Hase, F. Q. H. Ngo, and L. Kevan, *ibid.*, **62**, 985 (1975); (f) J. N. Helbert, B. E. Wagner, E. H. Poindexter, and L. Kevan, *J. Polym. Sci., Polym. Phys. Ed.*, **13**, 825 (1975).
(9) P. A. Narayana, M. K. Bowman, D. Becker, L. Kevan, and R. N. Schwartz, *J. Chem. Phys.*, **67**, 1990 (1977).
(10) J. Helbert, Ph.D. Thesis, Wayne State University, 1972.
(11) (a) M. K. Bowman, Ph.D. Thesis, Wayne State University, 1975; (b) M. K. Bowman and L. Kevan, *J. Phys. Chem.*, **81**, 456 (1977).
(12) J. S. Hyde, G. H. Rist, and L. E. G. Eriksson, *J. Phys. Chem.*, **72**, 4269 (1968).
(13) D. S. Leniart, J. S. Hyde, and J. C. Vedrine, *J. Phys. Chem.*, **76**, 2079 (1972).
(14) J. C. Vedrine, J. S. Hyde, and D. S. Leniart, *J. Phys. Chem.*, **76**, 2087 (1972).
(15) V. L. Hochman, V. Ya. Zevin and B. D. Shanina, *Fiz. Tverd. Tela*, **10**, 337 (1968); *Sov. Phys.-Solid State (Engl. Trans).*, **10**, 269 (1968).
(16) A. G. Redfield, *Phys. Rev.*, **98**, 1787 (1955).
(17) P. A. Narayana, D. Becker, and L. Kevan, *J. Chem. Phys.*, in press.
(18) B. C. Gerstein, C. Chow, R. G. Pembleton, and R. C. Wilson, *J. Phys. Chem.*, **81**, 565 (1977).
(19) T. Yokono and Y. Sanada, private communication.
(20) K. Toriyama, K. Nunome, and M. Iwasaki, *J. Chem. Phys.*, **64**, 2020 (1976).
(21) D. L. VanderHart and H. L. Retcofsky, *Fuel*, **55**, 202 (1976).
(22) G. A. Mills, *Ind. Eng. Chem.*, **61**, 6 (1969).

Pressure Saturation of the Collisional Quenching of the $^3B_1$ State of SO_2

S. J. Strickler* and R. Neil Rudolph

Contribution from the Department of Chemistry, University of Colorado, Boulder, Colorado 80309. *Received August 19, 1977*

Abstract: Direct measurements are reported of the lifetime of the $^3B_1$ state of SO_2 at pressures from 8 to 1300 Torr, and in the presence of N_2, CO_2, and H_2O at varying pressures. It is shown that the collisional quenching saturates at higher pressures, approaching a limiting rate of about 1.3×10^6 s^{-1}. Two models are proposed to account for this effect: one a theory of radiationless transitions, and one a kinetic scheme involving other triplet states. The models predict different pressure dependences. The data favor the kinetic model, but are not good enough to distinguish definitely between the two.

I. Introduction

The spectra and lifetime of the $^3B_1$ state of sulfur dioxide have been of interest for some time. One reason is that this state is probably involved in atmospheric photochemistry of some importance.[1,2] Another reason is that the SO_2 molecule and this state in particular have been important in the development of theories of radiationless transitions in small molecules.[3-6]

The collisional quenching of the $^3B_1$ state by ground-state SO_2 and a number of other gases has been measured. These have generally been discussed in terms of the following types of processes:

$$^3SO_2 \xrightarrow{k_p} SO_2 + h\nu \quad (1)$$

$$^3SO_2 + M_i \xrightarrow{k_{qi}} SO_2 + M_i \quad (2)$$

In some studies at low pressures a pressure-independent nonradiative decay

$$^3SO_2 \xrightarrow{k_{nr}} SO_2 \quad (3)$$

has also been considered,[3] although other studies[7,8] have indicated it to be less important and theoretical considerations suggest that there should be no such process at the limit of zero pressure. In addition, some gases react chemically with the $^3B_1$ state of SO_2, and equations must be included to describe the

0002-7863/78/1500-3326$01.00/0

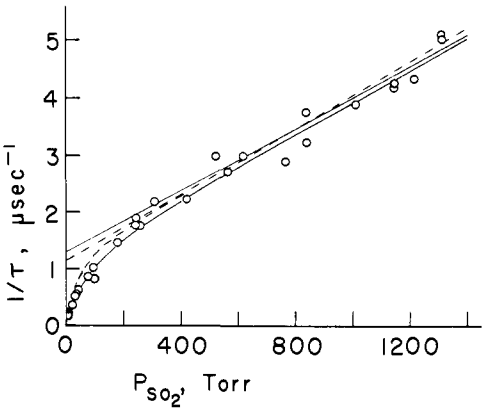

Figure 1. Phosphorescence decay rate of pure SO_2. The curved solid line is a least-squares fit to the data of eq 6 and the straight solid line is the resulting asymptote for this form. The dashed curve and straight line are a fit and resulting asymptote of eq 19.

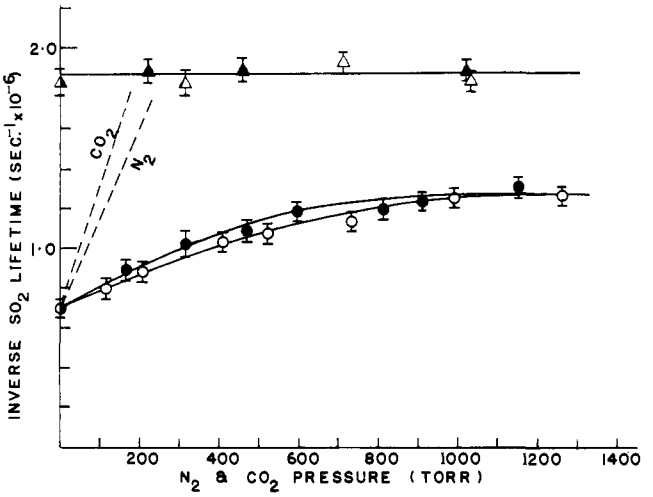

Figure 2. Phosphorescence decay rate of SO_2 with addition of N_2 and CO_2. Circles represent the addition of gas to 45 Torr SO_2 and triangles represent the addition of gas to 250 Torr SO_2. Solid figures are addition of CO_2 and open figures are addition of N_2. The dashed lines show slopes calculated from low-pressure rate constants.[2]

reactions. For example, ground-state SO_2 reacts according to the equation[9]

$$^3SO_2 + SO_2 \xrightarrow{k_c} SO_3 + SO \qquad (4)$$

There have been two basic types of study of collisional quenching of the $^3B_1$ state. One type is an actual lifetime study, and the other type is a study of quantum yields of emission or of the products of reactions, either chemical reactions or energy transfer. In either case, data obtained as a function of pressure have generally been interpreted in terms of equations like 1-4 by making Stern-Volmer graphs of the results. At relatively low pressures, say up to 20 Torr, the data appear to fit the expected Stern-Volmer behavior quite well. However, deviations have been noted at higher pressures. For example, Calvert and co-workers have noted lifetimes that seemed too long[10] and quantum yields that seemed too high[11,12] at higher pressures. They attributed the effect to the participation of another unknown precursor state X of SO_2. Heicklen and co-workers[13] also found some reaction quantum yields that were unexpectedly large at higher pressures, and invoked two additional precursor excited states of SO_2 to account for their data.

We present here a direct study of the decay rate of the $^3B_1$ state of SO_2 at relatively high pressures of SO_2 and of N_2 and CO_2, and, in addition, with H_2O vapor at pressures up to about 20 Torr. The observed lifetimes are longer than expected from Stern-Volmer behavior. We interpret our results, not in terms of other precursor states, but in terms of pressure saturation of collisional quenching. Such behavior has been predicted theoretically by Freed.[14] We discuss the theoretical implications of our observations.

II. Experimental Section

Total emission spectra of SO_2 have been measured for pressures up to 1 atm at room temperature of 24 ± 2 °C. Excitation was by light from a high-pressure mercury lamp passed through a Bausch and Lomb high-intensity monochromator, a Corning 7-54 filter, and 1 cm of a saturated solution of $NiSO_4$. The emission was observed at right angles by a Jarrell-Ash 0.75-m spectrograph with an EMI 6256S photomultiplier tube. The sample cell was a 1-cm rectangular quartz fluorescence cell attached to a Teflon stopcock. At high pressures of SO_2 most of the absorption and subsequent emission occurs very close to the window where the exciting light enters the cell, so the cell was positioned with that face very close to the spectograph slit.

Lifetime measurements were made using a single photon counting technique.[15] The excitation source was a free-running spark lamp in air. Molecular nitrogen emission lines centered around 3159 Å were selected by a monochromator, giving a light pulse of a few nanoseconds duration. The sample was in a 1-cm rectangular fluorescence cell, and its emission was viewed through an interference filter with a band-pass of 760 Å centered at 4373 Å. This permitted good separation of the SO_2 phosphorescence from scattered light and other interferences. A few lifetimes were measured with excitation at other wavelengths, especially 2960 Å, and a few with a double Woods-horn cell, but the results were the same as with the above conditions. Further details of the apparatus may be found elsewhere.[16]

The gases were handled on greaseless vacuum systems. Pressures less than 250 Torr were measured with a Texas Instruments Bourdon gauge, higher pressures with a U-tube mercury manometer. A typical run required about 6 h to accumulate enough photon counts to give good statistics. The resulting decay curves were analyzed by a weighted least-squares procedure.

III. Results and Discussion

Total emission spectra of SO_2 gas as a function of pressure were reported by Strickler and Howell.[4] Their studies indicated that the intensities of both fluorescence and phosphoresence increased at low pressures but leveled off by about 1 Torr. Their kinetic analysis, based on processes like 1-4, would suggest that the ratio of fluorescence to phosphorescence intensity should remain constant at higher pressures. Our spectra show this not to be the case. Instead, the phosphorescence intensity grows relative to the fluorescence until the latter becomes essentially undetectable. This increase in triplet emission is analogous to the "excess triplet" observed by Calvert and co-workers.[12] The total emission spectrum at pressures above 100 Torr appears identical with that observed at lower pressures using a phosphoroscope.[17] No other emission can be detected within the range of our photomultiplier tube, i.e., at $\lambda < 6500$ Å. Addition of foreign gases does not alter the shape of the spectrum. Addition of 1200 Torr of N_2 to 300 Torr of SO_2 has no effect on the phosphorescence intensity.

Figure 1 shows the decay rate of the phosphorescence as a function of pressure in pure SO_2 gas. Pressures ranged from 8 to 13 Torr. The initial slope of the curve is in good agreement with the slope measured at low pressures by other workers, but deviations from Stern-Volmer behavior are apparent on this pressure scale, and the curve bends over and approaches a straight line of much smaller slope. A few measurements of lifetime at high pressures were made using excitation directly into the triplet region at 3577 and 3371 Å. The errors are large owing to the low intensity, but the lifetimes appear to be the same as those obtained by excitation in the singlet region.

Figure 2 shows the decay rate when varying pressures of N_2 and CO_2 are added to a fixed partial pressure of SO_2 gas. The

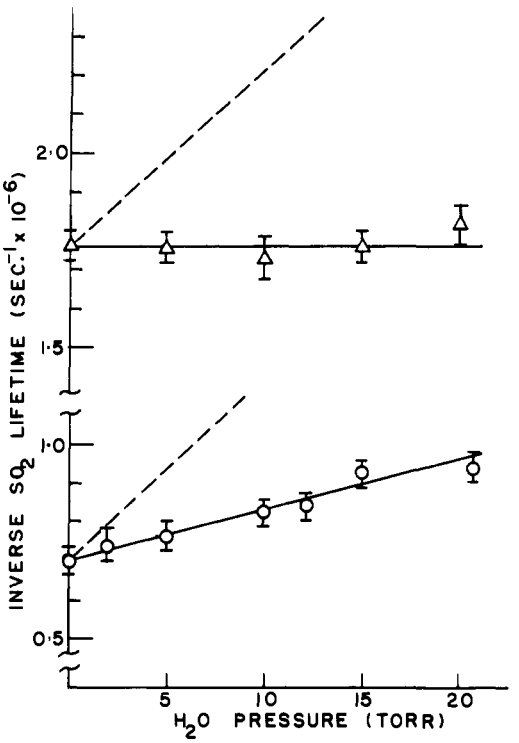

Figure 3. Phosphorescence decay rate of SO_2 with addition of H_2O. Circles represent the addition of H_2O to 45 Torr SO_2 and triangles represent the addition of H_2O to 250 Torr SO_2. The dashed lines show the slopes calculated from low-pressure rate constants.[2]

lower curves are for 45 Torr of SO_2. The dashed lines indicate the slopes expected from the low-pressure quenching rates. Clearly, the initial slopes are much smaller than expected, and the curves gradually level off and become nearly horizontal. This represents the pressure saturation. It may be noted that, although the initial slopes are slightly different for N_2 and CO_2, the final level reached seems to be essentially the same. The upper curves in Figure 2 show measurements at 250 Torr of SO_2. It appears that pressure saturation has already occurred at that SO_2 pressure, and the addition of these inert gases has essentially no further effect on decay rate. Figure 3 shows comparable results for water vapor. These are restricted to pressures below the vapor pressure of water, but otherwise the results are similar.

Interpretation of Results

Our interpretation of these results is as follows. In the case of pure SO_2 gas, the processes which need to be considered are eq 1, 2, and 4. The usual kinetic treatment can be applied to the first-order emission (eq 1) and to the second-order chemical reaction (eq 4). However, process 2, a physical quenching, shows pressure saturation. The pseudo-first-order rate constant for disappearance of $^3SO_2$ in process 2 seems to be fairly well represented by the simplest form of expression having the right asymptotic behavior:

$$k_{qSO_2}P_{SO_2}/(1 + k_{qSO_2}P_{SO_2}) \quad (5)$$

This expression reduces to $k_{qSO_2}P_{SO_2}$ at low pressure, and to a constant, $1/\alpha$, at high pressure. The total pseudo-first-order rate constant may then be written as

$$k = k_p + k_cP_{SO_2} + k_{qSO_2}P_{SO_2}/(1 + \alpha k_{qSO_2}P_{SO_2}) \quad (6)$$

Under high-pressure conditions k_p makes a negligible contribution to k, although it is only because of the existence of the k_p that we can observe the triplet decay. Our data do not give a value for k_p; the value calculated from absorption intensity[5] is 79 s^{-1}, and the best experimental value[8] about 120 s^{-1}. A least-squares fit of eq 6, neglecting k_p, to the data reported here for the decay of pure SO_2 gives $k_c = 2.72 \times 10^3$ s^{-1} $Torr^{-1}$ = 5.04×10^7 L mol^{-1} s^{-1}, $k_{qSO_2} = 1.94 \times 10^4$ s^{-1} $Torr^{-1}$ = 3.60×10^8 L mol^{-1} s^{-1}, and $\alpha = 7.73 \times 10^{-7}$ s or $1/\alpha = 1.29 \times 10^6$ s^{-1}. These may be compared with other values in the literature. For example, Chung, Calvert, and Bottenheim[9] measured the rate of reaction 4 and obtained $k_c = (4.2 \pm 0.4) \times 10^7$ L mol^{-1} s^{-1}, in fair agreement with our value. The sum of k_c and k_{qSO_2} should be the slope of the low-pressure Stern–Volmer plot of decay rate vs. pressure. From the above values $k_c + k_{qSO_2}$ = 2.21×10^4 s^{-1} $Torr^{-1}$ = 4.10×10^8 L mol^{-1} s^{-1}. Several literature values are available for this quantity. Sidebottom et al.[18] obtained $(3.9 \pm 0.1) \times 10^8$ L mol^{-1} s^{-1}, Strickler et al.[5] obtained $(4.52 \pm 0.18) \times 10^8$ L mol^{-1} s^{-1}, Briggs et al.[7] obtained $(4.46 \pm 0.11) \times 10^8$ L mol^{-1} s^{-1}, and recent measurements by Su et al.[8] give $(4.2 \pm 0.1) \times 10^8$ L mol^{-1} s^{-1}, so our value is certainly reasonable. Calvert and co-workers[19] have also indicated some success in fitting the pressure saturation data with an expression like eq 5 with very similar results. Their value for $1/\alpha$, called K in their notation, is 1.5×10^6 s^{-1}.

N_2 and CO_2 are inert gases which appear to quench the $^3B_1$ state of SO_2 only by process 2. At low pressures the quenching by these gases is considerably less efficient than quenching by SO_2 molecules. The quenching would be expected to show pressure saturation just like quenching by SO_2, but should require higher pressures. This is exactly what is observed in Figure 2. At 45 Torr of SO_2 the quenching is already partly pressure saturated, so the initial slopes of the curves upon adding N_2 or CO_2 are lower than the low-pressure values. As the pressure increases the curves bend over and become nearly horizontal above about 1000 Torr. The initial slope for CO_2 is somewhat greater than for N_2, as are the low-pressure quenching rates, but the final limiting rate constants are indistinguishable. At 250 Torr of SO_2, the collisional quenching is already essentially pressure saturated and the addition of N_2 or CO_2 has no noticeable effect on the lifetime.

Figure 3 shows that the same appears to be true of quenching by H_2O, although the study cannot be extended to H_2O pressures high enough to give saturation at 45 Torr of SO_2. Thus in these experiments H_2O seems to take part only in process 2 and not in any significant chemical reaction. It should be noted, however, that in the presence of oxygen H_2O has an additional effect.[20]

We have studied quenching by O_2 and find that the effect of O_2 is much more complicated than that of N_2 or CO_2. The quenching does not show pressure saturation, but the actual effects depend on the pressure of SO_2 and H_2O present. We plan to discuss these effects elsewhere.

Theory of Collisional Quenching

In this section we propose two possible mechanisms for collisional quenching which would lead to a pressure saturation. The first involves a theoretical treatment of radiationless transitions from the $^3B_1$ state to the ground state. The other is a kinetic scheme involving other triplet states. The two models predict different variations with pressure, and these will be compared with experimental observations.

Radiationless Transition Model. A theory of collision-induced intersystem crossing has been developed by Freed[14] and applied by him to explain observations on glyoxal.[21] His theory predicts that, under certain conditions, the collisional quenching will show a pressure saturation. The pressure at which this should become important depends on ρ, the density of vibrational levels of the final state in the neighborhood of the initial state. Use of Haarhoff's formula[22] gives a density of 0.67 levels per cm^{-1} at this energy; a direct counting of levels using the anharmonic molecular constants of Shelton et al.[23] gives a density of 0.7–0.8 levels per cm^{-1}. If it is assumed that 10% of hard sphere collisions are effective in producing rota-

tional relaxation, Freed's theory predicts that saturation should become important at around 50 Torr. This certainly agrees qualitatively with our observations.

We present here a much simpler treatment than that of Freed, which makes the physical basis more transparent and gives a definite prediction of the pressure dependence. It does not seem to be quite equivalent to Freed's theory, but is more restrictive in its applicability. It probably applies only to rather small molecules.

Let us consider a particular rovibronic level of the $^3B_1$ state. Close by, with an energy separation Γ, will be some highly excited level of the ground state with the same total angular momentum which can interact with the $^3B_1$ level with some intramolecular coupling matrix element β. Let us assume that at some time $t_e = 0$ the molecule is in the $^3B_1$ level, which we will call an initial state, and consider only those two levels. We can then use simple time-dependent perturbation theory[24] to write the probability of being in the ground-state level as a function of elapsed time t_e as

$$\frac{4\beta^2}{4\beta^2 + \Gamma^2} \sin^2 \frac{(4\beta^2 + \Gamma^2)^{1/2}}{2\hbar} t_e \tag{7}$$

If there is more than one ground-state level which interacts with the initial level, this expression will not be exact, but it will be nearly correct if the probability of being in the initial state is always close to unity, which will be the case if $\beta \ll \Gamma$ for all levels. If there is one level with small Γ, the expression will work for that level but not for others; however, most of the effect will then be due to that nearby level and the others will be unimportant anyway. The calculation would break down if there were more than one ground state level with a Γ which was not much larger than β. If we restrict ourselves to cases with $\beta \ll 1/\rho$, where ρ is the density of levels of the final state, we can use expression 7 to give the probability of being in each level of the ground state.

Now collisions can produce a rotational relaxation of the molecule. The cross section for rotational relaxation may be different from a gas kinetic cross section, but we can assume that there is some frequency Z of effective collisions. If the molecule is in one of the ground-state levels, then an effective collision will cause relaxation to another ground-state level, which will result in quenching of the triplet state and rapid return to the lower levels of the ground state. The probability that the collision will do this is just given by expression 7. If the molecule is not in one of the ground-state levels, but is in the original triplet-state level, the relaxation will go to some other rovibronic level of the triplet state. This new initial level will have its own set of ground-state levels with which it can interact, presumably at different energy separations, and it will also then evolve in a way represented by expression 7.

A triplet SO_2 molecule at pressures above 1 Torr will suffer at least 300 hard sphere collisions per mean life, so there should be an effective averaging over many rotational and vibrational levels. Some will have nearly degenerate ground-state levels; most will not. However, we should average over the different levels, which means averaging over the distribution of Γ's. The probability of finding a ground-state level at an energy separation between Γ and $\Gamma + d\Gamma$ is simply $\rho d\Gamma$. Furthermore, we must look at the probability of various elapsed times between collisions, and average over them. At a given collision the probability that the last collision occurred between t_e and $t_e + dt_e$ earlier is $Ze^{-Zt_e}dt_e$. Then the probability p that an effective collision will find the molecule in a ground-state level and result in quenching is given by

$$p = \int_{-\infty}^{\infty} d\Gamma \int_0^{\infty} dt_e Z e^{-Zt_e} \rho \times \frac{4\beta^2}{4\beta^2 + \Gamma^2} \sin^2 \frac{(4\beta^2 + \Gamma^2)^{1/2}}{2\hbar} t_e \tag{8}$$

which gives

$$p = \frac{2\pi\beta^2\rho}{(\hbar^2 Z^2 + 4\beta^2)^{1/2}} \tag{9}$$

The pseudo-first-order rate constant for collisional quenching is obtained by multiplying p by the frequency of effective collisions, Z.

$$k = \frac{2\pi\beta^2\rho Z}{(\hbar^2 Z^2 + 4\beta^2)^{1/2}} \tag{10}$$

At low pressures this reduces to

$$k = \pi\beta\rho Z \tag{11}$$

which is proportional to pressure, and at high pressures it reduced to a constant rate

$$k = 2\pi\beta^2\rho/\hbar \tag{12}$$

which is just the value given by Fermi's golden rule.

Because eq 11 and 12 have different dependences on β, it is possible to estimate both β and ρ from the low-pressure slope and the high-pressure asymptote. If we make the assumption that every gas-kinetic, hard-sphere collision is effective in causing rotational relaxation, we estimate $\beta = 1.3 \times 10^{-3}$ cm^{-1} and $\rho = 0.64$ levels per cm^{-1}. The latter is in good agreement with the level densities estimated above, and we see no reason for arguing against the value of β, so the model as a whole seems reasonable.

Kinetic Model. We present here an entirely different model to describe the quenching in terms of collisional interconversion of different triplet states. The spectrum of the ground state to $^3B_1$ transition has been analyzed in some detail by Merer and co-workers.[25] A series of perturbations have been ascribed to interactions with a $^3A_2$ state lying about 300 cm^{-1} higher in energy than the $^3B_1$ state, but with a very different geometry, in particular having a bond angle of about 97°. Calculations[26,27] have suggested that a $^3B_2$ state lies even lower in energy than the $^3B_1$, and also at an angle of around 100°.

We suggest the following kinetic scheme.

$$SO_2(^3B_1) + M \underset{k_{-1}}{\overset{k_1}{\rightleftharpoons}} SO_2(^3A_2) + M \tag{13}$$

$$SO_2(^3A_2) \xrightarrow{k_F} SO_2(^3B_2) + h\nu \tag{14}$$

We assume the $^3B_2$ state to return to the ground state by some unspecified mechanism. A standard kinetic treatment, using a steady-state approximation for the concentration of the $^3A_2$ state, results in the following expression for the pseudo-first-order rate constant for decay of the $^3B_1$ state:

$$k = \frac{k_1 k_F[M]}{k_F + k_{-1}[M]} \tag{15}$$

At low pressures this reduces to

$$k = k_1[M] \tag{16}$$

and at high pressures to

$$k = (k_1/k_{-1})k_F \tag{17}$$

If we assume that k_1/k_{-1}, the equilibrium constant for the production of the $^3A_2$ state from the $^3B_1$ state, is given by $\exp(-300 \text{ cm}^{-1}/kT) = 0.23$, and set k of eq 17 equal to $1/\alpha$ of eq 6, we find that k_F must be about 5.6×10^6 s^{-1}, which is about the sort of rate expected for a transition which is symmetry and spin allowed but not especially strong. Thus the kinetic model also seems to offer a reasonable explanation for the collisional quenching.

Comparison of Models. Both the radiationless transition model and the kinetic model discussed above seem to offer a

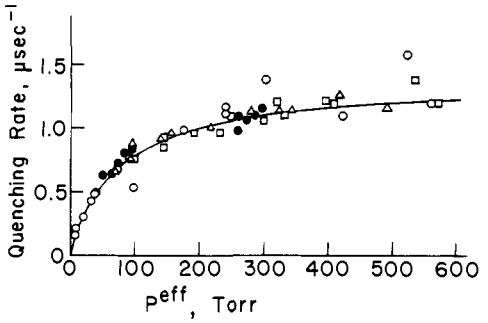

Figure 4. Rate of phosphorescence quenching for SO_2. P^{eff} is defined in the text. Open circles are for pure SO_2, squares are for addition of N_2, triangles are for addition of CO_2, and solid circles are for addition of H_2O. The solid line is the curve of eq 5 with constants obtained by fitting all of our data.

reasonable qualitative explanation of the observed pressure saturation of collisional quenching, i.e., both predict quenching to be proportional to pressure at low pressures but to approach a constant rate at high pressures. However, the two models predict different variations at intermediate pressures. The kinetic model gives a pressure variation of the form $k = k_qP/(1 + \alpha k_qP)$, identical with the empirical expression 5, where $k_q = k_1$ and $1/\alpha = (k_1/k_{-1})k_F$. The radiationless transition model predicts the form

$$k = \frac{k_qP}{(1 + \alpha^2k_q^2P^2)^{1/2}} \quad (18)$$

where $k_q = \pi\beta\rho(Z/P)$ and $1/\alpha = 2\pi\beta^2\rho/\hbar$. Compared to the behavior predicted by eq 5, for the same initial slope k_q and asymptotic value $1/\alpha$, eq 18 predicts that the decay rate should follow the Stern–Volmer line until somewhat higher pressures, and then bend over more suddenly toward the asymptotic value.

Figure 1 shows the pressure variation predicted by both models. The solid curve shows a plot of eq 6 with the constants obtained by a least-sqaures fit to our data as mentioned above. This is the form expected from the kinetic model. The solid straight line is the asymptotic form $k = k_cP + 1/\alpha$ which would be obtained if the quenching were completely saturated and only the chemical reaction varied with pressure. The dashed curve is a plot of the analogous equation for the radiationless transition model:

$$k = k_p + k_cP_{SO_2} + k_{qSO_2}P_{SO_2}/(1 + \alpha^2k^2_{qSO_2}P_{SO_2}{}^2)^{1/2} \quad (19)$$

A least-squares fit of eq 19 to our data gives a good fit, but the initial slope obtained in that way is too low to be consistent with the measurements made at low pressures by other workers. We have therefore chosen the constants in a farily arbitrary manner, taking the initial slope to be $k_c + k_{qSO_2} = 2.1 \times 10^4$ s^{-1} $Torr^{-1} = 3.9 \times 10^8$ L mol^{-1} s^{-1}, and choosing the other constants for a reasonable fit.

Unfortunately, our data are not good enough to distinguish between these two models. The maximum difference between the two predictions occurs in the region from about 50 to 200 Torr. In this region the kinetic model gives a definitely better fit to the data, but probably not so much better as to eliminate the other mechanism. The observation by Otsuka and Calvert[28] of a temperature dependence of the total quenching rate in SO_2 gas and the observation by Meyer et al.[29] of long triplet lifetimes in condensed phases at low temperatures are also more easily explained by the kinetic model.

Effect of Inert Gases. Both the models predict that the effect of adding other, nonreactive gases should be to affect only the quenching process 2, and move it toward saturation. Other gases might be more or less efficient than SO_2 in giving rotational relaxation (radiationless transition model) or in giving transitions between the $^3B_1$ and $^3A_2$ states (kinetic model). However, the final saturation rate of process 2 should be the same for any inert gas. This suggests that we could define an effective pressure of any gas as $P_M{}^{eff} = P_M(k_{qM}/k_{qSO_2})$, where the k_q's are low-pressure quenching rate constants, and that, if we plot the quenching rate as a function of this effective pressure, the data for all quenching gases should fall on the same curve.

Figure 4 shows such a plot for all of our data for effective pressures up to 600 Torr. For SO_2 we have subtracted from the observed $1/\tau$ the value of $k_cP_{SO_2}$ using our least-squares value of k_c in the kinetic model equation. The values of k_{qM} used to obtain effective pressures were (in units of 10^8 L mol^{-1} s^{-1}) 3.5, 0.85, 1.14, and 8.9 for SO_2, N_2, CO_2, and H_2O, respectively. The first of these is our present value; the others are from the work of Sidebottom et al.[2] The solid line is a plot of the equation

$$k = \frac{k_qP^{eff}}{1 + \alpha k_qP^{eff}} \quad (20)$$

where $P^{eff} = \Sigma_M P_M{}^{eff}$, $k_q = 1.89 \times 10^4$ s^{-1} $Torr^{-1}$, and $\alpha = 7.26 \times 10^{-7}$ s are the values obtained from a least-squares fit to all of our data, including those with quenching gases. We have used the form of equation given by the kinetic model because of the somewhat better fit. The fit of the radiationless transition model is not quite as good, but again the data involving other gases are not good enough to distinguish definitely between the two models.

The kinetic model proposed here is specific to quenching of the $^3B_1$ state of SO_2. It requires the existence of another state at a comparable energy, which can be equilibrated with the former by collisions, and it requires a rapid, pressure-independent path for removal of the other state. The observed $^3A_2$ and calculated $^3B_2$ states provide a plausible explanation for the effect. On the other hand, the radiationless transition model is more general, and should be applicable to other small molecules, whether or not it is the correct explanation in the case of SO_2. We are attempting to test the models by improving our experimental accuracy on lifetimes in the critical pressure region, and by searching for the infrared emission of eq 14. We are also looking for similar effects in other molecules.

Whatever the explanation, the experiments make it quite certain that the collisional quenching of the $^3B_1$ state does show pressure saturation. This has some important applications to the lifetime of this state in the atmosphere.[20] It also appears to help explain some previous results on pressure dependence of lifetimes and quantum yields.[8]

Acknowledgments. This work was supported by the National Science Foundation. The authors would like to thank Professor J. G. Calvert for preprints of his work and for informative conversations, and Dr. L. E. Brus and Professor K. F. Freed for their comments.

References and Notes

(1) R. S. Berry and P. A. Lehman, *Annu. Rev. Phys. Chem.*, **32**, 47 (1971).
(2) H. W. Sidebottom, C. C. Badcock, G. E. Jackson, J. G. Calvert, G. W. Reinhardt, and E. K. Damon, *Environ. Sci. Technol.*, **6**, 72 (1972).
(3) A. E. Douglas, *J. Chem. Phys.*, **45**, 1007 (1966).
(4) S. J. Strickler and D. B. Howell, *J. Chem. Phys.*, **49**, 1947 (1968).
(5) S. J. Strickler, J. P. Vikesland, and H. D. Bier, *J. Chem. Phys.*, **60**, 664 (1974).
(6) W. M. Gelbart and K. F. Freed, *Chem. Phys. Lett.*, **18**, 470 (1973).
(7) J. P. Briggs, R. B. Caton, and M. J. Smith, *Can. J. Chem.*, **53**, 2133 (1975).
(8) F. Su, J. W. Bottenheim, D. L. Thoresell, J. G. Calvert, and E. K. Damon, *Chem. Phys. Lett.*, **49**, 305 (1977).
(9) K. Chung, J. G. Calvert, and J. W. Bottenheim, *Int. J. Chem. Kinet.*, **7**, 161 (1975).
(10) F. B. Wampler, J. G. Calvert, and E. K. Damon, *Int. J. Chem. Kinet.*, **5**, 107 (1973).
(11) F. B. Wampler, A. Horowitz, and J. G. Calvert, *J. Am. Chem. Soc.*, **94**, 5523

(1972).
(12) A. Horowitz and J. G. Calvert, *Int. J. Chem. Kinet.*, **5**, 243 (1973).
(13) E. Cehelnik, C. W. Spicer, and J. Heicklen, *J. Am. Chem. Soc.*, **93**, 5371 (1971).
(14) K. F. Freed, *J. Chem. Phys.*, **64**, 1604 (1976).
(15) A. E. W. Knight and B. K. Selinger, *Aust. J. Chem.*, **26**, 1 (1973).
(16) M. J. Boyd, Ph.D. Thesis, The University of Colorado, Boulder, Colo., 1975.
(17) J. P. Vikesland and S. J. Strickler, *J. Chem. Phys.*, **60**, 660 (1974).
(18) H. W. Sidebottom, C. C. Badcock, J. G. Calvert, G. W. Reinhardt, B. R. Rabe, and E. K. Damon, *J. Am. Chem. Soc.*, **93**, 2587 (1971).
(19) F. Su, F. B. Wampler, J. W. Bottenheim, D. L. Thorsell, J. G. Calvert, and E. K. Damon, *Chem. Phys. Lett.*, **51**, 150 (1977).
(20) R. N. Rudolph and S. J. Strickler, *J. Am. Chem. Soc.*, **99**, 3871 (1977).
(21) K. F. Freed, *Chem. Phys. Lett.*, **37**, 47 (1976).
(22) P. C. Haarhoff, *Mol. Phys.*, **7**, 101 (1963).
(23) R. D. Shelton, A. H. Nielson, and W. H. Fletcher, *J. Chem. Phys.*, **21**, 2178 (1953); **22**, 1791 (1954).
(24) G. W. Robinson and R. P. Frosch, *J. Chem. Phys.*, **37**, 1962 (1962).
(25) A. J. Merer, private communication. Also Symposium on Molecular Spectroscopy, Columbus, Ohio, June 14, 1976, paper WC7.
(26) I. H. Hillier and V. R. Saunders, *Mol. Phys.*, **22**, 193 (1971).
(27) D. D. Lindley, H. L. Hsu, R. M. Pitzer, and I. Shavitt, Symposium on Molecular Spectroscopy, Columbus, Ohio, 1976, paper WC10. Also private communication from I. Shavitt.
(28) K. Otsuka and V. R. Calvert, *J. Am. Chem. Soc.*, **93**, 2581 (1971).
(29) B. Meyer, L. F. Phillips, and J. J. Smith, *Proc. Natl. Acad. Sci. U.S.A.*, **61**, 7 (1968).

Determination of the Absolute Configuration of a Secondary Hydroxy Group in a Chiral Secondary Alcohol Using Glycosidation Shifts in Carbon-13 Nuclear Magnetic Resonance Spectroscopy

Shujiro Seo, Yutaka Tomita, Kazuo Tori,* and Yohko Yoshimura

Contribution from Shionogi Research Laboratory, Shionogi & Co., Ltd., Fukushima-ku, Osaka, 553, Japan. *Received August 15, 1977*

Abstract: A new method is proposed for determining the absolute configuration of a secondary hydroxy group in a chiral secondary alcohol using glycosidation shifts in ^{13}C NMR spectroscopy. The ^{13}C FT NMR spectra of a number of secondary alcoholic glucopyranosides in pyridine-d_5 were compared with those of methyl glucosides and the corresponding parent alcohols to obtain the glucosidation shifts; $\Delta\delta_S$ = δ(alcoholic glucoside) − δ(methyl glucoside) for sugar moieties and $\Delta\delta_A$ = δ(alcoholic glucoside) − δ(alcohol) for aglycone moieties. Characteristic $\Delta\delta_S$(C-1′), $\Delta\delta_A$(C-α), and $\Delta\delta_A$(C-β) values were obtained for the various kinds of secondary alcohols. They are summarized as a few rules for determining the absolute configuration of the hydroxyl.

In a recent review dealing with the conformational properties of glycosidic linkages, Lemieux and Koto[1] reported that ^{13}C chemical shifts around glycosidic linkages depend upon conformations thereabout based on investigations of ^{13}C NMR spectra of cyclohexyl α- and β-D-glucopyranosides and their *C*-methyl derivatives in connection with conformational analyses. During studies of structural determinations and ^{13}C FT NMR spectral signal assignments of natural plant glycosides,[2] Tanaka and co-workers[3] and we[4] also found that ^{13}C NMR signal shifts in the change from aglycone alcohol and pyranose into glycopyranoside, that is, glycosidation shifts,[2] are characteristic of chemical and steric environments of the hydroxy group in which the glycosidation takes place. This discovery has become important and useful for determining the glycosidation position in an aglycone moiety and the kind(s) and sequence of sugar moiety present in a natural glycoside without chemical degradation as well as for assigning ^{13}C NMR signals of the glycoside.[5]

Among several glycosidation shifts, the shift difference between signals due to two β carbons (see Figure 1) in chiral secondary alcoholic glycosides appears to be the most practical to use for determining the absolute configuration of the secondary hydroxy group in a chiral secondary alcohol. As a result of further extension of our study, we propose here a new ^{13}C NMR method for determining the absolute configuration of the secondary hydroxy group mentioned above.

Experimental Section

Materials. All the D-glucopyranosides and tetra-*O*-acetyl-D-glucopyranosides used were prepared by the Koenigs–Knorr method,[6] and their properties are listed in Table I.

Measurements of NMR Spectra. Natural-abundance ^1H noise-decoupled ^{13}C FT NMR spectra were recorded on a Varian NV-14 FT NMR spectrometer at 15.087 MHz using 8-mm spinning tubes. Samples of all alcohols examined were dissolved in both pyridine-d_5 and chloroform-d, whereas those of glucopyranosides and their peracetates were measured in pyridine-d_5 and chloroform-d, respectively. Tetramethylsilane (Me_4Si) served as an internal reference (δ 0). Samples of small-sized molecules were measured at ambient probe temperature (30 °C), while those of large-sized molecules were examined at elevated temperatures (100 °C in pyridine-d_5 and 80 °C in chloroform-d) to avoid signal broadenings on the 15-MHz spectrometer. Concentrations were about 0.1–0.5 mmol/cm^3. FT NMR measurement conditions were as follows: spectral width, 3923 Hz; pulse flipping angle, 15–30° according to molecular size; acquisition time, 0.6 s; number of data points, 4820. Accuracies of δ values were thus about ±0.1. The calibration of the spectrometer was checked by using the δ value of the carbonyl carbon resonance (171.50) of methyl acetate (82% v/v) in benzene-d_6 (10% v/v) and Me_4Si (8% v/v) ac-

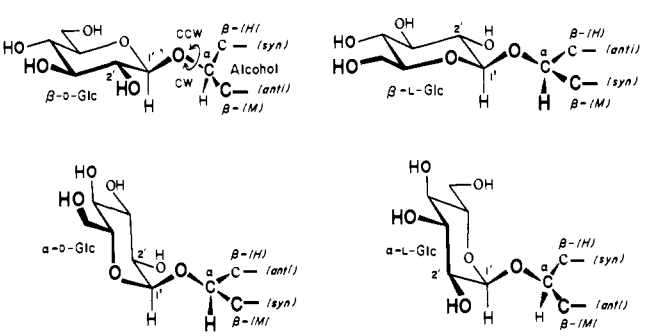

Figure 1. Conformations around glucosidic linkages.[1]

0002-7863/78/1500-3331$01.00/0